

Measurement of the Thermal Diffusivity of an Anisotropic Graphite Sheet Using a Laser-Heating AC Calorimetric Method¹

H. Nagano,^{2,3} H. Kato,⁴ A. Ohnishi,⁵ and Y. Nagasaka⁶

The thermal diffusivity of a graphite sheet having an extremely high anisotropy has been measured by a laser heating AC calorimetric method in the temperature range from 30 to 350 K. This graphite sheet has characteristics of high thermal diffusivity and high anisotropy, and it is only 100 μm thick. Thus, it is difficult to apply the conventional AC technique. Therefore, we propose a simultaneous measurement method for the in-plane and out-of-plane thermal diffusivities, by analyzing the three-dimensional heat conduction process, which contains the effects of anisotropy and thermal wave reflections. This method was verified by checking with thermal diffusivity measurements of isotropic materials such as stainless steel and pure copper and was then applied to the anisotropic thermal diffusivity measurement¹ of the graphite sheet.

KEY WORDS: anisotropy; graphite sheet; high thermal diffusivity; laser-heating AC calorimetric method; simultaneous measurement.

1. INTRODUCTION

We have proposed a high thermal conductive graphite sheet (GS) for a spacecraft thermal control application. The GS, which has been developed

¹ Paper presented at the Fourteenth Symposium on Thermophysical Properties, June 25–30, 2000, Boulder, Colorado, U.S.A.

² Graduate School of Science and Technology, Keio University, 3-14-1, Hiyoshi, Yokohama 223-8522, Japan.

³ To whom correspondence should be addressed.

⁴ National Research Laboratory of Metrology, 1-1-4, Umezono, Tsukuba, Ibaraki 305-8563, Japan.

⁵ Institute of Space and Astronautical Science, 3-1-1, Yoshinodai, Sagami-hara, Kanagawa 229-8510, Japan.

⁶ Department of System Design Engineering, Keio University, 3-14-1, Hiyoshi, Yokohama 223-8522, Japan.

by Matsushita Electric Industrial Co., Ltd., is a two-dimensional orthotropic material. We have measured both the in-plane and out-of-plane thermal diffusivities by a laser-heating AC calorimetric method [1–3]. In the present AC technique, a modulated laser beam, which is focused, is irradiated upon a sample surface, and the phase lag of the thermal wave is detected by a fine thermocouple [4]. The in-plane thermal diffusivity is determined by the slope of the relation of the phase lag vs the relative distance between the heating point and the detection point, and the out-of-plane thermal diffusivity is calculated by the phase lag vs the modulating frequency.

In the case of the GS measurement, the following features of the GS must be taken into account.

- (1) *GS has a high thermal diffusivity in the in-plane direction.* If the thermal diffusivity of the sample is high, the measured thermal diffusivity deviates significantly from the true value due to the effects of the thermal wave reflections at the edges of the sample. Gu et al. [5] report a theoretical study of the effect of the first reflection at the edge in the light scanning direction (x direction). However, in the present system, we need to consider the reflections in several directions repeatedly due to the high thermal diffusivity of the GS.
- (2) *GS is a thin material (100 μm thick).* In a thin sample, the size of the silver paste to attach the thermocouple to the sample becomes relatively large, resulting in a contribution to the phase lag measurement. Hatta et al. [6] report that there is no effect of the silver paste on the in-plane measurement because the heat capacity of the silver paste does not affect the slope of phase lag vs distance. However, in the out-of-plane measurement, the effect of silver paste cannot be neglected because the degree of the effect of silver paste is changed in accordance with the modulating frequency. Therefore, by an AC technique, out-of-plane thermal diffusivity measurement has been limited to a poorly thermal diffusive material and/or a thick material [7].

In the present paper, we propose a new method to determine both the in-plane and the out-of-plane thermal diffusivities simultaneously by analyzing the three-dimensional heat conduction process, which contains the effects of thermal wave reflections and anisotropic thermal diffusivity. The three-dimensional AC temperature response for an anisotropic plate-like sample is numerically estimated using Green's function. The applicability of the simultaneous measurement method to the AC technique was tested at room temperature by using isotropic materials such as stainless steel and

pure copper. In addition, this method was applied to the anisotropic thermal diffusivity measurement of the graphite sheet in the temperature range from 30 to 350 K.

2. THEORETICAL ANALYSIS

First, consider a homogeneous medium of three-dimensional infinite extent. When a point heat source is liberated at the rate $\rho c e^{i\omega t}$ at the point (x', y', z') , where ρ is the average density of the medium and c is the heat capacity, the propagation of thermal waves in a three-dimensional infinite region can be expressed as [8]

$$T_{ac}(x, y, z, t) = \frac{1}{4\pi a l(x, y, z)} \exp[-kl(x, y, z) + i\{\omega t - kl(x, y, z)\}] \quad (1)$$

where T_{ac} is the AC temperature at the detection point (x, y, z) , $\omega = 2\pi f$ is the angular frequency, and a is the thermal diffusivity. l is the distance between the heat source and the detection point and can be written

$$l(x, y, z) = \sqrt{(x - x')^2 + (y - y')^2 + (z - z')^2} \quad (2)$$

k is the thermal wave number, defined as

$$k = \sqrt{\frac{\pi f}{a}} = \mu^{-1} \quad (3)$$

where μ is the thermal diffusion length. The detected phase lag $\Delta\phi$ of the thermal wave is given by

$$\Delta\phi(x, y, z) = -kl(x, y, z) \quad (4)$$

Second, consider a three-dimensional orthotropic medium of the three-dimensional infinite region. Green's function at x at time t due to the unit instantaneous heat source at x' at time t' is

$$G_x(x, t; x', t') = \frac{1}{2\sqrt{\pi a_x(t-t')}} \left\{ \exp\left(-\frac{(x-x')^2}{4a_x(t-t')}\right) \right\} \quad (5)$$

where a_x is the thermal diffusivity in the x direction. Green's functions at y and z can be written as the same configuration with thermal diffusivities a_y and a_z . The AC temperature response is expressed as

$$\begin{aligned}
 T_{ac}(x, y, z, t) &= \int_{-\infty}^t e^{i\omega t} G_x(x, t; x', t') G_y(y, t; y', t') G_z(z, t; z', t') dt' \\
 &= \frac{e^{i\omega t}}{4\pi \sqrt{a_y a_z} l'(x, y, z)} \\
 &\quad \times \exp[-k_x l'(x, y, z) + i\{\omega t - k_x l'(x, y, z)\}] \quad (6)
 \end{aligned}$$

where

$$l'(x, y, z) = \sqrt{\frac{a_x}{a_x} (x - x')^2 + \frac{a_x}{a_y} (y - y')^2 + \frac{a_x}{a_z} (z - z')^2}, \quad k_x = \sqrt{\frac{f}{a_x}} \quad (7)$$

Final, let us consider a three-dimensional orthotropic medium of the semiinfinite region as shown in Fig. 1a, with a width w along the y axis, a thickness d along the z axis, and an infinite length along the x axis, where the length is longer than the scanning length and thermal diffusion length. The detected AC temperature is the sum of the thermal wave propagated from the point heat source directly and the waves which are reflected at the edges of the sample and then reach the detection point. When the point heat source is located at (x', y', z') , the thermal wave in the y direction is reflected at $(x', y' \pm w/2, z')$. Furthermore, thermal waves are reflected repeatedly at reciprocal edges. One can consider these reflected waves as thermal waves propagated from an imaginary heat source at $(x', y' \pm mw, z')$ as shown in Fig. 1b [9]. The same assumption is adapted to the z direction as shown in Fig. 1c. Green's function in the z direction is expressed as

$$\begin{aligned}
 G_z(z, t; z', t') &= \frac{1}{2\sqrt{\pi a_z(t-t')}} \left[\exp\left(-\frac{(z-z')^2}{4a_z(t-t')}\right) + \exp\left(-\frac{(z+z')^2}{4a_z(t-t')}\right) \right. \\
 &\quad + \sum_{n=1}^{\infty} \gamma^{2n-1} \left\{ \exp\left(-\frac{[z-(z'+2nd)]^2}{4a_z(t-t')}\right) + \exp\left(-\frac{[z+(z'+2nd)]^2}{4a_z(t-t')}\right) \right\} \\
 &\quad \left. + \sum_{n=1}^{\infty} \gamma^{2n} \left\{ \exp\left(-\frac{[z-(z'-2nd)]^2}{4a_z(t-t')}\right) + \exp\left(-\frac{[z+(z'-2nd)]^2}{4a_z(t-t')}\right) \right\} \right] \quad (8)
 \end{aligned}$$

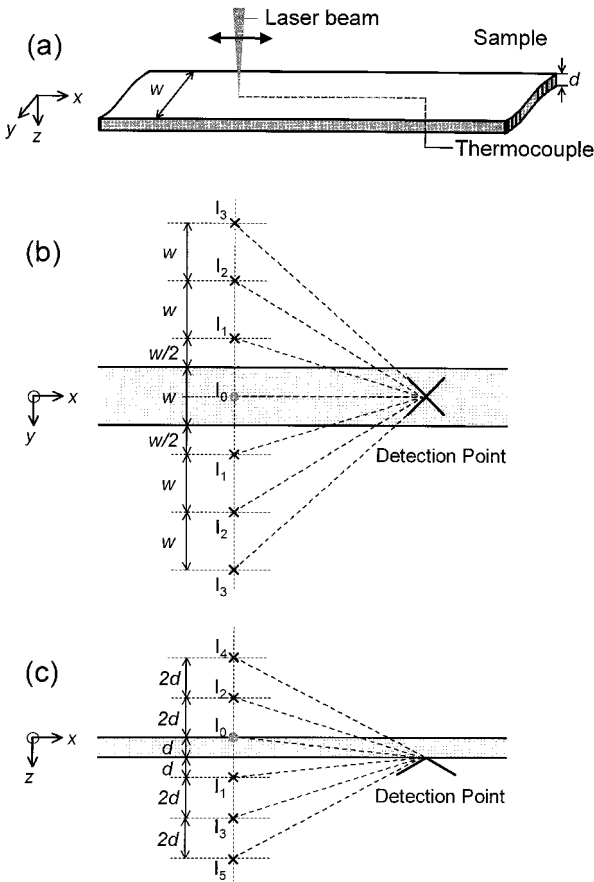


Fig. 1. Sample shape for thermal diffusivity measurement (a) and mirror images of the point heat source in the y direction (b) and in the z direction (c).

where γ is the thermal wave reflectance at the sample–exterior interface defined by [10]

$$\gamma = \frac{e_s - e_e}{e_s + e_e} \quad (9)$$

where e_s and e_e are the thermal effusivities of the sample and the exterior, respectively. When the laser beam is irradiated at point $(0, 0, 0)$, the AC temperature response is written

$$\begin{aligned}
T_{ac}(x, y, z, t) = & \frac{e^{i\omega t}}{4\pi \sqrt{a_y a_z}} \left[2 \frac{e^{-(1+i)kl''(0,0)}}{l''(0,0)} + 2 \sum_{m=1}^{\infty} \gamma^m \left\{ \frac{e^{-(1+i)kl''(m,0)}}{l''(m,0)} \right\} \right. \\
& + \sum_{n=1}^{\infty} \gamma^{2n-1} (\gamma + 1) \left\{ \frac{e^{-(1+i)kl''(0,n)}}{l''(0,n)} \right\} \\
& \left. + \sum_{n=1}^{\infty} \sum_{m=1}^{\infty} \gamma^{2n+m-1} (\gamma + 1) \left\{ \frac{e^{-(1+i)kl''(m,n)}}{l''(m,n)} \right\} \right] \quad (10)
\end{aligned}$$

where

$$l''(m, n) = \sqrt{x^2 + \frac{a_x}{a_y} (mw)^2 + \frac{a_x}{a_z} [(2n+1)d]^2} \quad (11)$$

In the present measurement system, the experiment is performed in a vacuum, and so the thermal wave reflectance γ is equal to 1. Additionally, GS is a two-dimensional orthotropic material and has a homogeneous structure in the $x - y$ directions (i.e., $a_x = a_y \equiv a_{xy}$). The phase lag detected at $(x, 0, d)$ is obtained from

$$\begin{aligned}
\Delta\phi(x, y, z) = \text{Tan}^{-1} \frac{\left(\sum_{n=0}^{\infty} \langle [(e^{-kl''(0,n)}/l''(0,n)) \sin\{kl''(0,n)\}] \right. \\
\left. + 2 \sum_{m=1}^{\infty} [(e^{-kl''(m,n)}/l''(m,n)) \sin\{kl''(m,n)\}] \right)}{\left(\sum_{n=0}^{\infty} \langle [(e^{-kl''(0,n)}/l''(0,n)) \cos\{kl''(0,n)\}] \right. \\
\left. + 2 \sum_{m=1}^{\infty} [(e^{-kl''(m,n)}/l''(m,n)) \cos\{kl''(m,n)\}] \right)} \quad (12)
\end{aligned}$$

For the most precise measurements, the constant phase delay due to the effect of a silver paste is added to Eq. (12). The in-plane thermal diffusivity and the out-of-plane thermal diffusivity are determined simultaneously by the curve-fitting method, which is based on a simplex algorithm [11], where the complete $\Delta\phi$ vs x curve is fitted by Eq. (12).

3. VERIFICATION TEST USING ISOTROPIC MATERIALS

Verification of the new method is evaluated by checking the thermal diffusivities of stainless steel (Standard Reference Material, SRM1461), which were obtained from the NIST, and pure copper at room temperature. The detailed construction and operation of the apparatus are given in Refs. 2 and 4. This apparatus permits in-plane thermal diffusivity measurements with an uncertainty of not more than $\pm 3.0\%$ [4]. The sample shape, experimental conditions, and reference values for SRM1461 [12]

Table I. Shape of Samples and Experimental Conditions

Sample	Thickness (mm)	Shape (mm)	Frequency (Hz)	Scanning length (mm)	Reference value ($\text{mm}^2 \cdot \text{s}^{-1}$)
SRM1461	0.5	ϕ 12	2.11	2.0	3.72 [12]
Pure copper	0.1	12 \times 12	28, 33	0.4	117 [13]

and pure copper [13] are listed in Table I. Figure 2 shows the $\Delta\phi$ vs x/d results for SRM1461 and pure copper with fitting curves from Eq. (12). The deviations of the phase lag for the experiments from Eq. (12) are shown in Fig. 3. The deviations are generally less than $\pm 0.4\%$.

The in-plane and out-of-plane thermal diffusivities of SRM1461 and pure copper analyzed by curve fitting are listed in Table II with the in-plane thermal diffusivity calculated from the slope in region b in Fig. 2. The in-plane thermal diffusivities a_{xy} of stainless steel and pure copper obtained from curve fitting and the slope are in good agreement with recommended values, within $\pm 2.6\%$. The out-of-plane thermal diffusivities a_z of stainless steel and pure copper were underestimated by about 11 and 52%, respectively.

The value of the out-of-plane thermal diffusivity is determined mainly

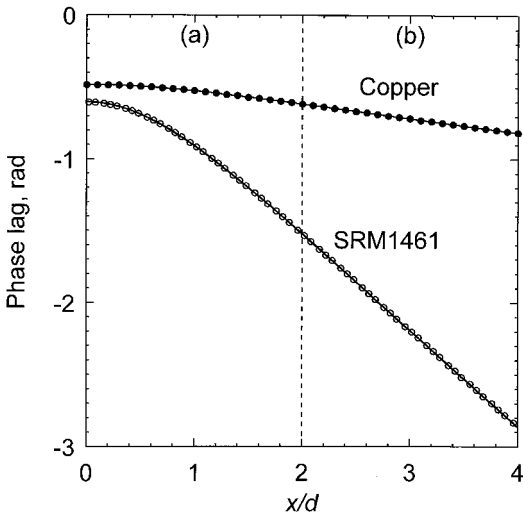


Fig. 2. Example of the measured phase lag vs non-dimensional distance and fitting curves of SRM1461 and pure copper.

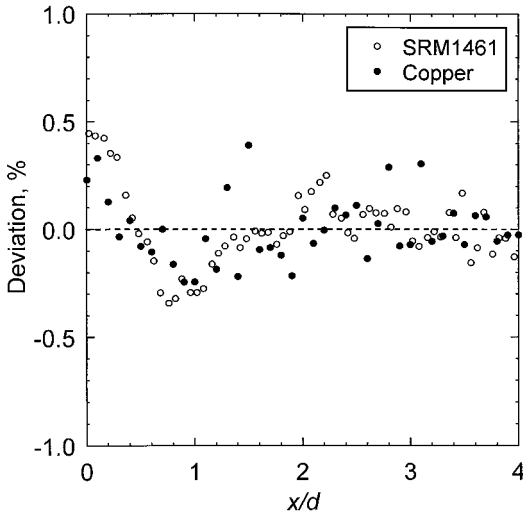


Fig. 3. Deviations of measured phase lag from fitting curves given by Eq. (12) of SRM1461 and pure copper.

by analyzing information from the $\Delta\phi$ vs x/d curve in region a in Fig. 2, which is called the “thickness effect.” Around the origin, however, the relative beam diameter becomes larger, and the assumption of the point heat source is not realized. That is why the out-of-plane thermal diffusivity has a larger uncertainty. Additionally, the degree of the thickness effect around the origin is determined by the thermal thickness, i.e., $(a_{xy}/a_z)d$ and thermal wave number k defined by Eq. (3). Both the thickness and the k value of the copper sample are smaller than those of the SRM1461 sample. That is why the pure copper sample shows a larger difference from the in-plane values than does the SRM1461. In the case of the GS, although the k value is smaller than that of pure copper and SRM1461 samples,

Table II. Thermal Diffusivity Values of Stainless Steel and Pure Copper Obtained from the Fitting Method and Slope

Sample	Frequency (Hz)	Fitting ($\text{mm}^2 \cdot \text{s}^{-1}$)		Slope (in-plane) ($\text{mm}^2 \cdot \text{s}^{-1}$)	SD (%)
		In-plane	Out-of-plane		
SRM1461	2.11	3.70	3.36	3.73	0.180
	2.11	3.69	3.28	3.69	0.089
Pure copper	28	119	57.4	114	0.078
	33	118	56.6	114	0.080

Table III. Shape of the GS Sample and Experimental Conditions

Sample	Thickness (mm)	Shape (mm)	Scanning length (mm)	Temperature (K)
Graphite sheet	0.1	7 × 40	4.0	30–350

the thermal thickness of the GS is larger than that of those samples due to its large anisotropy between the xy and the z directions. Therefore, the measured out-of-plane thermal diffusivity value of the GS would be underestimated by 11 to 52%.

4. RESULTS AND DISCUSSION

The sample shape of the GS and the experimental conditions for thermal diffusivity measurement are listed in Table III. A series of seven measurements was carried out over a range of modulating frequency from 5.2 to 95.4 Hz at room temperature. Figure 4 shows a typical example of

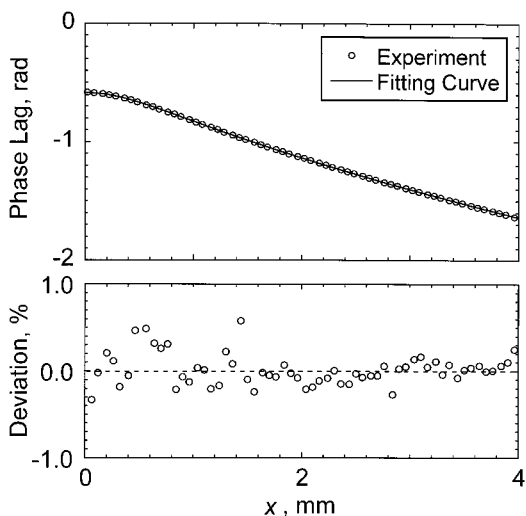


Fig. 4. Typical phase lag vs distance data and fitting curve given by Eq. (12) of the GS at room temperature. Deviation of the experimental data from fitting curve is displayed at the bottom.

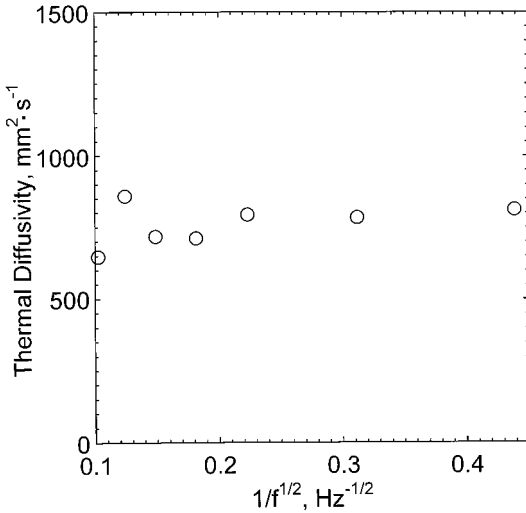


Fig. 5. Frequency dependence of effective thermal diffusivity for the GS at room temperature.

the $\Delta\phi$ vs x results and the fitting curve from Eq. (12) at 10.3 Hz. The deviation of the phase lag from the measurements with that given by Eq. (12), which is shown at the bottom of Fig. 4, is generally less than $\pm 0.5\%$. Figure 5 shows the frequency dependence of the effective thermal diffusivity obtained from the fitting method. The analyzed thermal diffusivity has approximately constant values in the range $0.22 < 1/f^{1/2} < 0.44$, which corresponds to a thermal diffusion length ranging from 3.5 to 7.0 mm and is regarded as the effective range. The average values of the in-plane and out-of-plane thermal diffusivities in the effective range at room temperature are determined to be $a_{xy} = 798 \text{ mm}^2 \cdot \text{s}^{-1}$ and $a_z = 15.7 \text{ mm}^2 \cdot \text{s}^{-1}$, respectively. The temperature dependence of the in-plane and out-of-plane thermal diffusivities in the temperature range from 30 to 350 K are shown in Fig. 6. It is clear that both the in-plane and the out-of-plane thermal diffusivities have a large temperature dependence. They have maximum values around 100 and 70 K, respectively. These values are approximately 7 and 10 times larger than the values at 350 K, respectively. Figure 7 shows the anisotropy ratio a_{xy}/a_z of the GS over the present temperature range. It is confirmed that the GS has extreme thermal anisotropy in the in-plane and out-of-plane directions. This ratio increases from 25 to 50 as the temperature increases, that is, the value of the in-plane thermal diffusivity is about 25 to 50 times larger than the out-of-plane result.

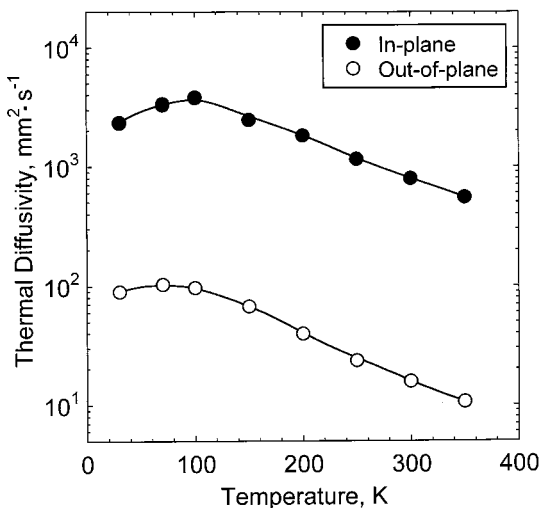


Fig. 6. Temperature dependence of the in-plane and out-of-plane thermal diffusivities of the GS.

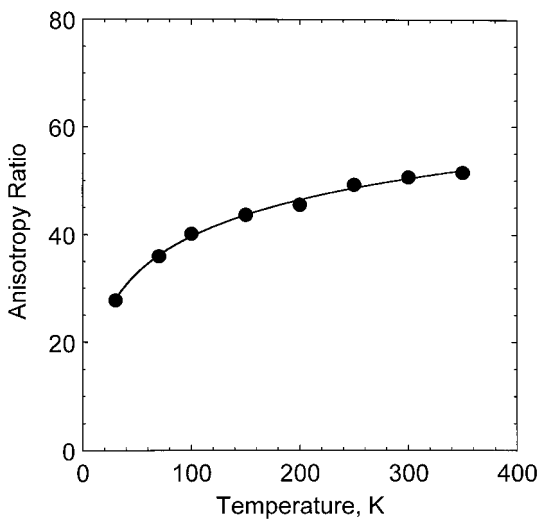


Fig. 7. Anisotropy ratio of in-plane thermal diffusivity to out-of-plane thermal diffusivity for the GS.

5. CONCLUSIONS

The results can be summarized as follows.

- (a) Simultaneous measurement of the in-plane and out-of-plane thermal diffusivities by a laser-heating AC calorimetric method has been proposed.
- (b) The three-dimensional AC temperature response for an anisotropic plate-like sample was numerically estimated using Green's function.
- (c) Verification of the measurement method is confirmed using isotropic materials at room temperature.
- (d) This method was applied to the graphite sheet measurement over the temperature range from 30 to 350 K, and a large temperature dependence and an extreme anisotropy of the thermal diffusivity have been determined quantitatively.

ACKNOWLEDGMENTS

We would like to acknowledge Mr. N. Nishiki of Matsushita Electric Industrial Co., Ltd., for supplying graphite sheets. We would also like to thank Dr. M. Okaji and Mrs. K. Tomoda of the National Research Laboratory of Metrology for much help during this research.

REFERENCES

1. H. Nagano, H. Kato, A. Ohnishi, N. Nishiki, and Y. Nagasaka, *Proc. 19th Jpn. Symp. Thermophys. Prop.*, Fukuoka, Japan (1998), pp. 247–250.
2. H. Nagano, H. Kato, A. Ohnishi, and Y. Nagasaka, *High Temp. High Press.* (in press).
3. H. Nagano, H. Kato, A. Ohnishi, N. Nishiki, and Y. Nagasaka, *Proc. 37th Natl. Heat Transf. Symp. Jpn.*, Kobe, Japan (May 2000).
4. H. Kato, *Proc. 20th Jpn. Symp. Thermophys. Prop.*, Tokyo (1999), pp. 400–403.
5. Y. Gu and I. Hatta, *Jpn. J. Appl. Phys.* **30**:1137 (1991).
6. I. Hatta, R. Kato, and A. Maezono, *Jpn. J. Appl. Phys.* **25**:L493 (1986).
7. T. Azumi, K. Takahashi, Y. Ichikawa, K. Motonari, and K. Yano, *Proc. 8th Jpn. Symp. Thermophys. Prop.*, Japan (1987), pp. 171–174.
8. H. S. Carslaw and J. C. Jaeger, *Conduction of Heat in Solids*, 2nd ed. (Oxford University Press, New York, 1959), p. 263.
9. H. Kato, K. Nara, and M. Okaji, *Proc. 4th Asian Thermophys. Prop. Conf.*, Tokyo (1995), pp. 581–584.
10. C. A. Bennett, Jr., and R. R. Patty, *Appl. Opt.* **21**:49 (1982).
11. J. A. Nelder and R. Mead, *Comp. J.* **7**:308 (1965).
12. S. H. Lee, T. Terai, and Y. Takahashi, *Jpn. J. Thermophys. Prop.* **8**:213 (1994).
13. Y. S. Touloukian, R. W. Powell, C. Y. Ho, and P. G. Klemens, *Thermophysical Properties of Matter 1* (IFI/PLENUM, New York, Washington, DC, 1970), p. 81.